

Dynamics of a Producer–Grazer Model Incorporating the Effects of Excess Food Nutrient Content on Grazer’s Growth

Angela Peace · Hao Wang · Yang Kuang

Received: 18 March 2014 / Accepted: 25 July 2014 / Published online: 15 August 2014
© Society for Mathematical Biology 2014

Abstract Modeling under the framework of ecological stoichiometric allows the investigation of the effects of food quality on food web population dynamics. Recent discoveries in ecological stoichiometry suggest that grazer dynamics are affected by insufficient food nutrient content (low phosphorus (P)/carbon (C) ratio) as well as excess food nutrient content (high P:C). This phenomenon is known as the “stoichiometric knife edge.” While previous models have captured this phenomenon, they do not explicitly track P in the producer or in the media that supports the producer, which brings questions to the validity of their predictions. Here, we extend a Lotka–Volterra-type stoichiometric model by mechanistically deriving and tracking P in the producer and free P in the environment in order to investigate the growth response of *Daphnia* to algae of varying P:C ratios. Bifurcation analysis and numerical simulations of the full model, that explicitly tracks phosphorus, lead to quantitative different predictions than previous models that neglect to track free nutrients. The full model shows that the fate of the grazer population can be very sensitive to excess nutrient concentrations. Dynamical free nutrient pool seems to induce extreme grazer population density changes when total nutrient is in an intermediate range.

Keywords Ecological stoichiometry · Producer–grazer model · Stoichiometric knife edge · Lotka–Volterra

A. Peace (✉) · Y. Kuang
School of Mathematical and Statistical Science, Arizona State University,
Tempe, AZ 85287-1804, USA
e-mail: angela.peace@asu.edu

H. Wang
Department of Mathematical and Statistical Sciences, University of Alberta,
Edmonton, AB T6G 2G1, Canada

1 Introduction

Low-nutrient food content causes a nutrient deficiency in grazers, the consequences of which are relatively well understood and modeled (Loladze et al. 2000; Elser et al. 2001; Demott et al. 1998; Frost et al. 2006). However, recent reported empirical data suggest that grazer dynamics are also affected by excess food nutrient content (Boersma and Elser 2006; Elser et al. 2006). This phenomenon, called the *stoichiometric knife edge*, reflects a reduction in animal growth not only by food with low P content but also by food with excessively high P content.

Understanding the issues of excess nutrients is especially important as human activities, such as mining phosphorus for agricultural uses such as fertilization and animal feed, continue to alter the global P cycle. Human-induced nutrient loads can be several magnitudes higher relative to natural levels (Elser and Bennett 2011; Smith and Schindler 2009). It has been shown that P accumulation and over enrichment of nutrients in terrestrial and aquatic systems can cause widespread problems (Bennett et al. 2001). P concentrations of freshwater systems worldwide are estimated to be at least 75% greater than preindustrial levels (Bennett et al. 2001; Gaxiola et al. 2011). Empirical data show that up to 10% of aquatic habitats have measurements of high algal P:C, in the range where grazer growth begins to decline due to excess P (Sterner et al. 2008).

Loladze et al. (2000) presented a two-dimensional Lotka–Volterra-type model (called the LKE model) of the first two trophic levels of a food chain (producer–grazer) incorporating the fact that both producers and grazers are chemically heterogeneous organisms. Specifically, it tracks the amount of two essential elements, carbon (C) and phosphorus (P), in each trophic level. It allows the phosphorus to carbon ratio (P:C) of the producer to vary above a minimum value. Below is the LKE model from Loladze et al. (2000):

$$\frac{dx}{dt} = bx \left(1 - \frac{x}{\min\{k, (P - \theta y)/q\}} \right) - f(x)y \quad (1a)$$

$$\frac{dy}{dt} = \hat{e} \min \left\{ 1, \frac{(P - \theta y)/x}{\theta} \right\} f(x)y - dy \quad (1b)$$

where $x(t)$ and $y(t)$ are the biomass of the producer and grazer, respectively, measured in terms of C, b is the maximum growth rate of producer, k is the producer carrying capacity in terms of C, or the light intensity, P is the total phosphorus in the system, θ is the grazer's constant P:C, q is the producer minimal P:C, \hat{e} is the maximum production efficiency, and d is the grazer loss rate. The grazer's ingestion rate, $f(x)$ is taken to be a monotonic increasing and differentiable function, $f'(x) \geq 0$, $f(0) = 0$. $f(x)$ is saturating with $\lim_{x \rightarrow \infty} f(x) = \hat{f}$. The model makes the following three assumptions.

A1: *The total mass of phosphorus in the entire system is fixed, i.e., the system is closed for phosphorus with a total of P (mg P/L).*

A2: *P:C ratio in the producer varies, but it never falls below a minimum q (mg P/mg C); the grazer maintains a constant P:C, θ (mg P/mg C).*

A3: All phosphorus in the system is divided into two pools: phosphorus in the grazer and phosphorus in the producer.

The LKE model also assumes the producer is optimal food for the grazer if its P:C ratio is equal to or greater than the P:C of the grazer, thus incorporating the effects of low-nutrient food content on grazer dynamics.

Elser et al. (2012) modified the LKE model to include the effects of excess nutrient content and incorporate the stoichiometric knife edge phenomenon. Peace et al. (2013) provided analysis of this two dimensional stoichiometric knife-edge model. This model assumed the mechanism behind this phenomenon is the grazer’s feeding behavior. It assumes that high P content of food causes the animal to strongly decrease their ingestion rate, perhaps leading to insufficient C intake and thus decreased growth rate. Below is the knife-edge model from Peace et al. (2013):

$$\frac{dx}{dt} = bx \left(1 - \frac{x}{\min\{k, (P - \theta y)/q\}} \right) - \min \left\{ f(x), \frac{\hat{f}\theta}{Q} \right\} y \tag{2a}$$

$$\frac{dy}{dt} = \min \left\{ \hat{e}f(x), \frac{Q}{\theta}f(x), \hat{e}\hat{f}\frac{\theta}{Q} \right\} y - dy \tag{2b}$$

where $Q = \frac{P-\theta y}{x}$. The model is parameterized for a producer–grazer system of algae (producer) and *Daphnia* (grazer). In addition to the three above assumptions, made by the LKE model, this model makes the following fourth assumption.

A4: The grazer ingests P up to the rate required for its maximal growth but not more.

The above assumption 3 presents a problem for the knife-edge model. It is assumed that all available P is in the algae; however, if the algae population is low, Q becomes unrealistically large. One possible approach to address this problem is to introduce a maximum value for Q . To improve this model, more work is needed to investigate this extreme scenario of excess P with low algal density and define a maximum for the producer P quota. Doing so would require an additional equation to handle free P concentrations. Here, we formulate a model to explicitly track free P in the stoichiometric knife-edge model following the procedure used by Wang et al. (2008). Our main goal of formulating this full model is to more accurately capture the grazer’s growth response to varying food quality in order to better understand the effects of nutrient levels on populations dynamics and food webs.

2 Model Construction

Let P_a describe the P in the algae, P_z the P in the zooplankton, and P_f the free P in the medium. We assume that total phosphorus, P, is constant.

$$P = P_a + P_z + P_f \tag{3}$$

Notice that P_a/x describes the producer cell quota. We assume that P_z/y , the grazer phosphorus content, remains constant. The following equations track the phosphorus in the algae and the free phosphorus.

$$\frac{dP_a}{dt} = \underbrace{v(P_f, Q)x}_{\text{P uptake}} - \underbrace{\frac{P_a}{x} \min \left\{ f(x), \frac{\hat{f}\theta}{P_a/x} \right\}}_{\text{P loss due to grazing}} y \tag{4}$$

$$\frac{dP_f}{dt} = \underbrace{-v(P_f, Q)x}_{\text{producer P uptake}} + \underbrace{\theta dy}_{\substack{\text{P from} \\ \text{grazer} \\ \text{death}}} + \underbrace{\min \left\{ f(x), \frac{\hat{f}\theta}{P_a/x} \right\} y \left(\frac{P_a}{x} - \min \left\{ \hat{\theta}, \frac{P_a/x}{\theta} \right\} \theta \right)}_{\text{P recycled by grazer}}; \tag{5}$$

Here, $v(P_f, Q)$ is the P uptake rate of the producer. This depends on the amount of available free phosphorus (P_f) as well as the producer quota (Q). As P_f increases, v should increase toward a carrying capacity, such as a Holling-type function response. Since Q is bounded above, v decreases as Q increases toward its maximum. v shall take the form following Diehl (2007),

$$v(P_f, Q) = \frac{\hat{c}P_f}{\hat{a} + P_f} \frac{\hat{Q} - Q}{\hat{Q} - q} \tag{6}$$

where \hat{Q} is the maximum Quota, \hat{c} is the maximum phosphorus per carbon uptake rate of the producer, and \hat{a} is the phosphorus half saturation constant of the producer.

There is a small modification in the producer equation. Under assumption 3, the previous model assumes $P - \theta y$ is the amount of P available for producer growth. To modify this to allow free P in the water, the amount of P available for producer growth is Qx . Therefore, the producer equation becomes

$$\frac{dx}{dt} = bx \left(1 - \frac{x}{\min(k, (Qx)/q)} \right) - \min \left\{ f(x), \frac{\hat{f}\theta}{Q} \right\} y. \tag{7}$$

Also note that

$$\frac{dx}{dt} = bx \min \left\{ 1 - \frac{x}{k}, 1 - \frac{x}{Qx/q} \right\} - \min \left\{ f(x), \frac{\hat{f}\theta}{Q} \right\} y \tag{8a}$$

$$= bx \min \left\{ 1 - \frac{x}{k}, 1 - \frac{q}{Q} \right\} - \min \left\{ f(x), \frac{\hat{f}\theta}{Q} \right\} y \tag{8b}$$

Letting $Q = P_a/x$, we can write an equation that described how the producer P quota changes over time.

$$\frac{dQ}{dt} = v(P_f, Q) - b \min \left\{ Q(1 - \frac{x}{k}), (Q - q) \right\} \tag{9}$$

We then arrive at the following model.

$$\frac{dx}{dt} = bx \min \left\{ 1 - \frac{x}{k}, 1 - \frac{q}{Q} \right\} - \min \left\{ f(x), \frac{\hat{f}\theta}{Q} \right\} y \tag{10a}$$

$$\frac{dy}{dt} = \min \left\{ \hat{e}f(x), \frac{Q}{\theta}f(x), \hat{e}\hat{f}\frac{\theta}{Q} \right\} y - dy \tag{10b}$$

$$\frac{dQ}{dt} = v(P_f, Q) - b \min \left\{ Q\left(1 - \frac{x}{k}\right), (Q - q) \right\} \tag{10c}$$

$$\frac{dP_f}{dt} = -v(P_f, Q)x + \theta dy + \min \left\{ f(x), \frac{\hat{f}\theta}{Q} \right\} y \left(Q - \min \left\{ \hat{e}, \frac{Q}{\theta} \right\} \theta \right) \tag{10d}$$

The assumption that total P in the system is constant allows this model to be reduced to three ODES. P is indeed constant, to see this conservation law note that total phosphorus can be expressed as $P = Q(t)x(t) + \theta y(t) + P_f(t)$. Then, since $\hat{e}f(x) < \hat{f}$, the following holds true.

$$\frac{dP}{dt} = Q'(t)x(t) + Q(t)x'(t) + \theta y'(t) + P'_f(t) \tag{11}$$

$$= \min \left\{ \hat{e}f(x), \frac{Q}{\theta}f(x), \hat{e}\hat{f}\frac{\theta}{Q} \right\} \theta y - \min \left\{ f(x), \frac{\hat{f}\theta}{Q} \right\} \min \left\{ \hat{e}, \frac{Q}{\theta} \right\} \theta y \tag{12}$$

$$= \min \left\{ \hat{e}f(x), \frac{Q}{\theta}f(x), \hat{e}\hat{f}\frac{\theta}{Q} \right\} \theta y - \min \left\{ \hat{e}f(x), \frac{Q}{\theta}f(x), \frac{\hat{e}\hat{f}\theta}{Q}, \hat{f} \right\} \theta y \tag{13}$$

$$= 0 \tag{14}$$

Thus, P is indeed constant, and we can formulate an expression for the free phosphorus, $P_f(t) = P - Q(t)x(t) - \theta y(t)$. The model may be reduced down to three equations.

$$\frac{dx}{dt} = bx \min \left\{ 1 - \frac{x}{k}, 1 - \frac{q}{Q} \right\} - \min \left\{ f(x), \frac{\hat{f}\theta}{Q} \right\} y \tag{15a}$$

$$\frac{dy}{dt} = \min \left\{ \hat{e}f(x), \frac{Q}{\theta}f(x), \hat{e}\hat{f}\frac{\theta}{Q} \right\} y - dy \tag{15b}$$

$$\frac{dQ}{dt} = v(P - Qx - \theta y, Q) - b \min \left\{ Q\left(1 - \frac{x}{k}\right), (Q - q) \right\} \tag{15c}$$

This full model (System 15), that explicitly tracks free phosphorus, is an extension of the two-dimensional knife-edge model (System 2) (Peace et al. 2013). The two-dimensional model (System 2) assumes the producer is extremely efficient at taking up free nutrients from the environment and that there is no upper bound for Q, as seen in assumption (A3). If we apply these assumptions to the full model (System 15), it converges to the previous model (System 2). To show this, first we consider System (15) and assume the producer has an infinite uptake efficiency ($\hat{c} \rightarrow \infty$). Then, the

dynamics of the producer P content are much faster than the growth dynamics of the populations and a quasi-steady state argument may be applied to Eq. (15c).

$$\begin{aligned}
 0 = \frac{dQ}{dt} &= \frac{\hat{c}(P - Qx - \theta y)}{\hat{a} + P - Qx - \theta y} \frac{\hat{Q} - Q}{\hat{Q} - q} - bQ \min \left\{ 1 - \frac{x}{K}, 1 - \frac{q}{Q} \right\} \\
 \implies (P - Qx - \theta y) \frac{\hat{Q} - Q}{\hat{Q} - q} &= \frac{bQ \min \left\{ 1 - \frac{x}{K}, 1 - \frac{q}{Q} \right\} (\hat{a} + P - Qx - \theta y)}{\hat{c}}
 \end{aligned}$$

Letting $\hat{c} \rightarrow \infty$ yields the following.

$$\begin{aligned}
 (P - Qx - \theta y) \frac{\hat{Q} - Q}{\hat{Q} - q} &= 0 \\
 (P - Qx - \theta y) \frac{1 - \frac{Q}{\hat{Q}}}{1 - \frac{q}{\hat{Q}}} &= 0
 \end{aligned}$$

Now we assume Q has no upper bound and let $\hat{Q} \rightarrow \infty$.

$$\begin{aligned}
 P - Qx - \theta y &= 0 \\
 \implies Q &= \frac{P - \theta y}{x}
 \end{aligned}$$

Equation (15a) can be written as

$$\begin{aligned}
 \frac{dx}{dt} &= bx \min \left\{ 1 - \frac{x}{k}, 1 - \frac{q}{(P - \theta y)/x} \right\} - \min \left\{ f(x), \frac{\hat{f}\theta}{Q} \right\} y \\
 &= bx \min \left\{ 1 - \frac{x}{k}, 1 - \frac{x}{(P - \theta y)/q} \right\} - \min \left\{ f(x), \frac{\hat{f}\theta}{Q} \right\} y \\
 &= bx \left(1 - \frac{x}{\min \{k, (P - \theta y)/q\}} \right) - \min \left\{ f(x), \frac{\hat{f}\theta}{Q} \right\} y
 \end{aligned}$$

and System (15) becomes equivalent to System (2). Hence, the two-dimensional knife-edge model can be regarded as the limiting case of the full model when $\hat{c} \rightarrow \infty$, $\hat{Q} \rightarrow \infty$.

3 Model Analysis

Here, we present a basic analysis on the model verifying the boundedness and positivity of the solutions. We also locate boundary equilibria and develop some criteria to determine their stability. Interior equilibria are investigated numerically in Sect. 4.1. For the following analysis, we denote $K = \min\{k, \frac{P}{q}\}$.

3.1 Positive Invariance

Theorem 3.1 *Solutions to System (15) with initial conditions in the set*

$$\Omega = \left\{ (x, y, Q) : 0 \leq x \leq K = \min \left\{ k, \frac{P}{q} \right\}, 0 \leq y, q \leq Q \leq \hat{Q}, Qx + \theta y \leq P \right\} \tag{16}$$

will remain there for all forward time.

Proof Let $S(t) = (x(t), y(t), Q(t))$ be a solution of System (15) with $S(0) \in \Omega$. Assume there exists a time $t_1 > 0$ such that $S(t_1)$ touches or crosses a boundary of Ω for the first time. The following cases prove the lemma by contradiction.

Case 1: $Q(t_1) = q$

Then, for every $t \in [0, t_1]$,

$$\begin{aligned} Q' &= v(P - Qx - \theta y, Q) - b \min \left\{ Q \left(1 - \frac{x}{k} \right), Q - q \right\} \\ &\geq -b \min \left\{ Q \left(1 - \frac{x}{k} \right), Q - q \right\} \\ &\geq -b(Q - q). \end{aligned}$$

This implies that $Q(t) \geq q + (Q(0) - q)e^{-bt} > q$. This contradicts $Q(t_1) = q$ and proves that $S(t_1)$ can not cross this boundary. The remaining cases follow similarly and are in Appendix 1. □

3.2 Boundary Equilibria

Consider the system,

$$x' = xF(x, y, Q) = 0 \tag{17a}$$

$$y' = yG(x, y, Q) = 0 \tag{17b}$$

$$Q' = H(x, y, Q) = 0 \tag{17c}$$

There are two equilibria on the boundary: E_0 for extinction of both the producer and the grazer and E_1 for extinction of just the grazer. $E_0 = (x_0, y_0, Q_0) = (0, 0, Q_0)$ where Q_0 satisfies $v(P, Q_0) = b(Q_0 - q)$. Although $Q_0 > 0$, this equilibrium still represents the case for producer and grazer extinction because $x_0, y_0 = 0$. $E_1 = (x_1, y_1, Q_1) = (k, 0, \min\{\frac{P}{k}, \hat{Q}\})$ if $1 - \frac{x}{k} < 1 - \frac{q}{Q}$ and $E_1 = (\frac{P}{q}, 0, q)$ if $1 - \frac{x}{k} > 1 - \frac{q}{Q}$. The following theorems give results on the stability of these extinction equilibria.

The Jacobian of the above system (17) is

$$J = \begin{vmatrix} F(x, y, Q) + xF_x(x, y, Q) & xF_y(x, y, Q) & xF_Q(x, y, Q) \\ yG_x(x, y, Q) & G(x, y, Q) + yG_y(x, y, Q) & yG_Q(x, y, Q) \\ H_x(x, y, Q) & H_y(x, y, Q) & H_Q(x, y, Q) \end{vmatrix}.$$

Theorem 3.2 *The producer and grazer extinction equilibrium, E_0 , is unstable.*

The proof is in Appendix 2.

Lemma 3.1 *The grazer extinction equilibrium $E_1 = (x_1, y_1, Q_1)$ takes the following form for the cases below.*

$$E_1 = (x_1, y_1, Q_1) = \begin{cases} \left(k, 0, \min\left\{\frac{P}{k}, \hat{Q}\right\}\right) & \text{if } 1 - \frac{x}{k} < 1 - \frac{q}{Q} \\ \left(\frac{P}{q}, 0, q\right) & \text{if } 1 - \frac{x}{k} > 1 - \frac{q}{Q} \end{cases} \quad (18)$$

and these two forms of E_1 cannot coexist.

The proof is in Appendix 3.

Theorem 3.3 *The grazer extinction equilibrium, E_1 , is locally asymptotically stable if*

$$\min \left\{ \hat{e}f(x_1), \frac{Q_1}{\theta}f(x_1), \hat{e}\hat{f}\frac{\theta}{Q_1} \right\} < d.$$

The proof is in Appendix 4.

Theorem 3.4 *The grazer extinction equilibrium, E_1 , is globally asymptotically stable if*

$$\min \left\{ \hat{e}f(K), \frac{\hat{Q}}{\theta}f(K), \hat{e}\hat{f}\frac{\theta}{q} \right\} < d.$$

The proof is in Appendix 5.

4 Numerical Experiments

This section describes the results of numerical experiments and a numerical bifurcation analysis on interior equilibria. All simulations use the Holling-type II function $f(x) = \frac{\hat{f}x}{a+x}$ for the grazer ingestion rate. Parameter values are listed in Table 1. All parameters are biologically realistic values obtained from Andersen (1997) and Urabe and Sterner (1996) and used by Loladze et al. (2000) and Peace et al. (2013). The values of \hat{c} and \hat{a} are used in Wang et al. (2008) and are within the same orders of magnitude as those found in Andersen (1997) and Diehl (2007).

In our numerical experiments, we increase P in an ecological meaningful range from 0.03 to 0.2 mg P/L. P is the total amount of phosphorus in the system and affects the P:C ratio of the producer (Q) and thus the growth dynamics of the grazer. Figure 1 shows numerical simulations of the full model for varying values of P using initial conditions: $x_0 = 0.5$, $y_0 = 0.25$, and $Q_0 = (P - \theta y_0)/x_0$. As P increases, the system exhibits stable coexistence equilibria, periodic cycles, and grazer extinction equilibria. Values of P that lead the system into limit cycles can affect the grazer’s chance of survival. The cycles are large in amplitude, which results in the grazer population spending significant periods of time with low populations near extinction,

Table 1 Model parameters

Parameter		Value
P	Total Phosphorus	0.03–0.2 mg P/L
b	Maximal growth rate of producer	1.2/day
d	Grazer loss rate	0.25/day
θ	Grazer constant P:C	0.03 mg P/mg C
q	Producer minimal P:C	0.0038 mg P/mg C
\hat{e}	Maximal production efficiency	0.8 (unitless)
k	Producer carrying capacity	1.5 mg C/L
\hat{f}	Maximal ingestion rate of the grazer	0.81/day
a	Half saturation of the grazer ingestion response	0.25 mg C/L
\hat{c}	Maximum P per C uptake rate of the producer	0.2 mg P/mg C/day
\hat{a}	Phosphorus half saturation constant of the producer	0.008 mg P/L
\hat{Q}	Maximum quota	2.5 mg P/mg C
$f(x)$	Grazer ingestion rate	$\left(\frac{cx}{a+x}\right)/d$

All parameters are biologically realistic values obtained from Andersen (1997) and Urabe and Sterner (1996) and used by Loladze et al. (2000) and Peace et al. (2013). The values of \hat{c} and \hat{a} are used in Wang et al. (2008) and are within the same orders of magnitude as those found in Andersen (1997) and Diehl (2007)

where they are sensitive to stochastic extinction. The amplitude of these limit cycles is much larger than those on the 2D knife model, System (2), that does not explicitly track free phosphorus in the media (Peace et al. 2013).

4.1 Numerical Bifurcation Analysis

Here, we provide a numerical analysis on the interior equilibria for varying values of total phosphorus, P . We fix all other parameters with values listed in Table 1 and the Holling-type II function $f(x) = \frac{\hat{f}x}{a+x}$ for the grazer ingestion rate. The below model is parameterized for populations of algae and *Daphnia*:

$$\frac{dx}{dt} = 1.2x \min \left\{ 1 - \frac{x}{1.5}, 1 - \frac{0.0038}{Q} \right\} - \min \left\{ \frac{0.81x}{0.25 + x}, \frac{0.0243}{Q} \right\} y \tag{19a}$$

$$\frac{dy}{dt} = \min \left\{ \frac{0.648x}{0.25 + x}, \frac{Q}{0.03} \frac{0.81x}{0.25 + x}, \frac{0.0194}{Q} \right\} y - 0.25y \tag{19b}$$

$$\frac{dQ}{dt} = \frac{0.2(P - Qx - 0.03y)}{0.008 + P - Qx - 0.03y} \frac{2.5 - Q}{2.4962} - 1.2 \min \left\{ Q \left(1 - \frac{x}{1.5} \right), (Q - 0.0038) \right\}. \tag{19c}$$

The phase space is

$$\Omega = \left\{ (x, y, Q) : 0 \leq x \leq \min \left\{ 1.5, \frac{P}{0.0038} \right\}, 0 \leq y, 0.0038 \leq Q \leq 2.5, Qx + 0.03y \leq P \right\}. \tag{20}$$

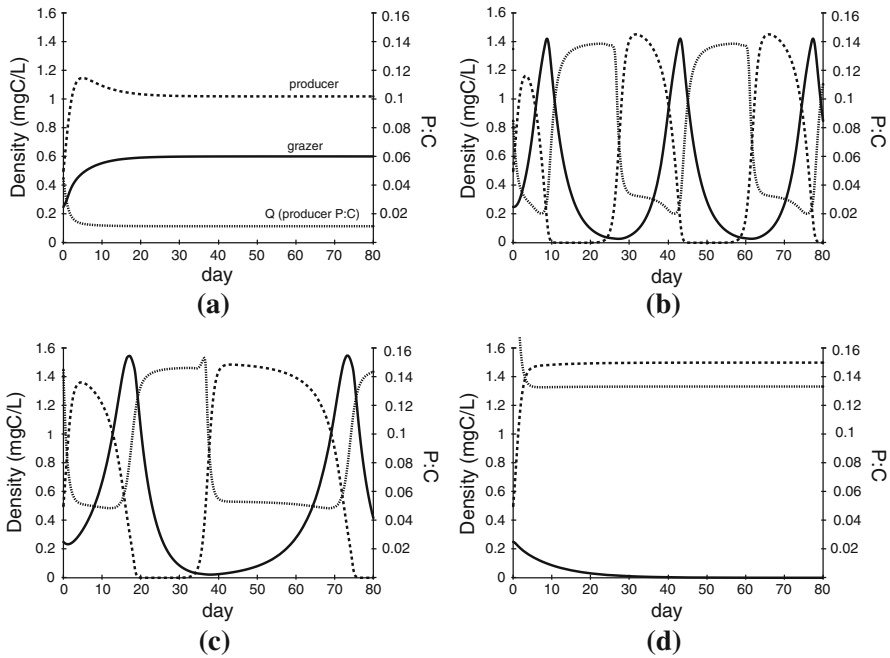


Fig. 1 Numerical simulations of the full model presented in System (15) performed using parameters found in Table 1 and varying values for P, **a** low total phosphorus $P = 0.03 \text{ mg P/L}$, **b** $P = 0.05 \text{ mg P/L}$, **c** $P = 0.08 \text{ mg P/L}$, **d** excess phosphorus $P = 0.2 \text{ mg P/L}$. $x_0 = 0.5 \text{ mg C/L}$, $y_0 = 0.25 \text{ mg C/L}$, $Q_0 = \min\{(P - \theta y_0)/x_0, \hat{Q}\}$ were used as initial conditions. Grazer and producer densities (mg C/L) are given by solid and big-dashed lines, respectively, and Q , producer cell quota (P:C), is given by small-dotted lines. **a** A positive stable equilibrium while **b** and **c** capture oscillations around unstable equilibria. These oscillations have an unstable grazer density, almost nearing extinction. **d** The grazer going toward extinction despite high food abundance. The extinction is caused by reduction in grazer growth due to high producer P:C

Now, we investigate the phase portraits for varying values of P. Figure 2 depicts the interior nullsurfaces of System (19). Notice the parameter P is only in the Q nullsurface. Therefore, varying P does not affect the x (blue) or y (yellow) nullsurfaces. Increasing P changes the Q (red) nullsurface. Equilibria are located where all three nullsurfaces intersect with each other.

The number of intersections, and thus the number of interior equilibria, depends on P. As P increases, simulations depict the Q nullsurface sweeping across the phase space and the number of intersections is either zero, one, two, or three. An animation of how the phase space changes for varying values of P is available as supplementary material (notes in 11). A bifurcation diagram is presented in Fig. 3. For low values of P ($P < 0.0163$), there is no intersection of all three nullsurfaces, as there is not enough P to support the *Daphnia* population (Fig. 2a). As P increases, initially there is only one intersection, a stable interior equilibrium. As P continues to increase, 3 equilibria appear: two unstable and one stable. One of the unstable equilibria and the stable equilibrium approach each other as P increases further. These two equilibria then converge and disappear at a saddle-node bifurcation ($P = 0.0319$), and a large

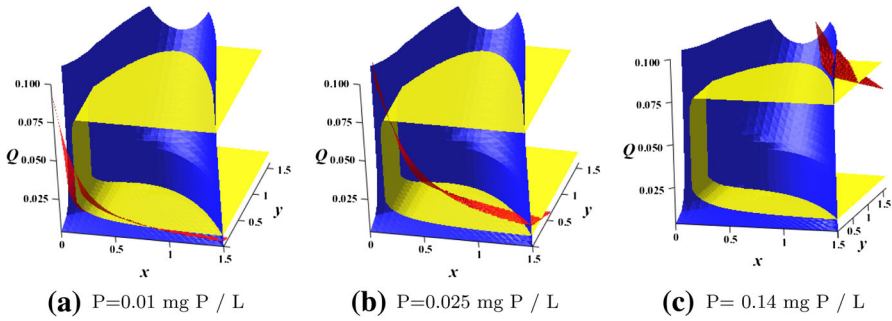


Fig. 2 Phase portraits of the full model presented in System (19) performed using parameters found in Table 1 and varying values for P , $P = 0.01$ mg P/L, $P = 0.025$ mg P/L, $P = 0.14$ mg P/L. The surfaces are the producer (blue), grazer (yellow), and producer P:C (red) nullsurfaces. The intersection of these surfaces depict equilibria. Varying P only affects the Q nullsurface (red) and changes the position and number of interior equilibria (Color figure online)

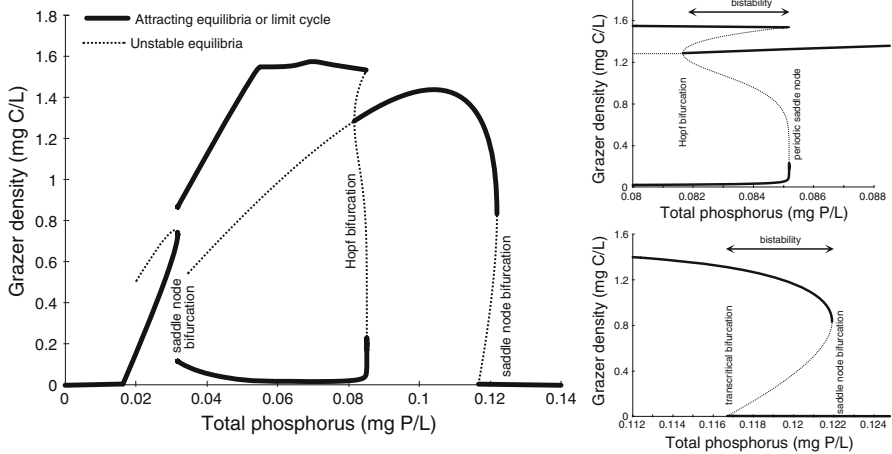


Fig. 3 Bifurcation diagram for the full model (System 15) using parameter values listed in Table 1. The bifurcation parameter, P , varies from 0 to 0.14 mg P/L. There are two saddle-node bifurcations, a Hopf bifurcation, a transcritical bifurcation, a periodic saddle-node bifurcation, and two regions of bistability. There is a stable equilibrium for low values of P . As P increases, the grazer equilibrium increases until the stable equilibrium loses its stability at a saddle-node bifurcation. There is a limit cycle, and as P increases, the amplitudes of the oscillations increase. For P large enough, the oscillations are abruptly halted at a periodic saddle-node bifurcation after the coexistence equilibrium is stabilized at a Hopf bifurcation and another coexistence equilibrium emerges. As P continues to increase, the grazer equilibria start to decrease until it reaches the second saddle-node bifurcation, and then, suddenly is driven to extinction. The right panels show closer views of the two regions of bistability. Data were generated using XPP-AUTO. The main qualitative behaviors of the bifurcation diagrams created by XPP-AUTO were similar when changing the minimum functions to their smooth analogs

amplitude limit cycle appears to be created. As P increases, the remaining unstable interior equilibrium is stabilized by a Hopf bifurcation ($P = 0.0815$). Immediately following this Hopf bifurcation, there is a brief region of bistability with the interior stable equilibrium and the limit cycles. As P continues to increase, this region of

bistability comes to an end via a periodic saddle-node bifurcation (“Blue sky” bifurcation) as the limit cycles disappear ($P = 0.0853$). After the collapse of the limit cycles, the one interior equilibrium remains stable. As P continues to increase, there is a transcritical bifurcation that restabilizes the grazer extinction boundary equilibrium and generates another interior equilibrium, which is unstable ($P = 0.1167$). Here, there is a second region of bistability with the stable interior equilibrium and the boundary grazer extinction equilibrium. Finally, as P increases to large enough values, the stable and unstable interior equilibria approach each other and converge at a saddle-node bifurcation ($P = 0.122$). Here, P is in excess, and we start to see the effects of the stoichiometric knife edge. The high levels of P lead to large enough algal P:C to lower the *Daphnia* density. Post this saddle-node bifurcation, there are no longer any intersections of all three nullsurfaces (Fig. 2c); thus, there are no interior equilibria. All solutions go to the boundary equilibria. Algal P:C is large enough to drive the *Daphnia* population to extinction. These are drastic effects of the stoichiometric knife edge phenomenon.

5 Discussion

The extended full knife-edge model (System 15), which mechanistically tracks P in the producer and free P in the environment, provides further investigations of the growth response of *Daphnia* to algae with varying P:C ratios. Section 2 shows that the full model (System 15) is an extension of the two-dimensional knife-edge model (System 2) (Peace et al. 2013). While the dynamics of these two models are similar, there are some important distinguishing features between these two models. A main qualitative difference between the knife-edge model System (2) and the full model System (15) can be seen when comparing the bifurcation diagrams, Fig. 4. In both diagrams, for very low values of P , the grazer cannot persist due to starvation. As P increases, the grazer equilibrium increases until the stable equilibrium loses its stability at a saddle-node bifurcation. There is a limit cycle, and as P increases, the amplitudes of the oscillations increase. For P large enough, the oscillations are abruptly halted when a Hopf bifurcation occurs and another coexistence equilibrium emerges. As P continues to increase, the grazer equilibria start to decrease and eventually is driven to extinction.

Differences between the two diagrams are first seen in the limit cycles. Oscillations in the full model (Fig. 4b) exhibit much larger amplitudes than those in the 2D model (Fig. 4a). These large limit cycles can be dangerous for the survival of the grazer. During these cycles, the grazer populations spend significant periods of time near low population values and are sensitive to stochastic extinction. Oscillations in both models are eventually halted after a Hopf bifurcation. The increase in food quantity accompanied by a decrease in food quality causes the flow of energy (C) from the producer to the grazer to decrease because the grazer is eating less biomass. Here, low food quality, due to excess P , drives these systems through the Hopf bifurcations. The location of the Hopf bifurcation is another important difference between these two models. The Hopf bifurcation of the 2D model occurs at a lower value of P making the region where cycling occurs shorter and the region for stable coexistence longer. In the full model, the Hopf bifurcation occurs at a higher value of P giving the grazer

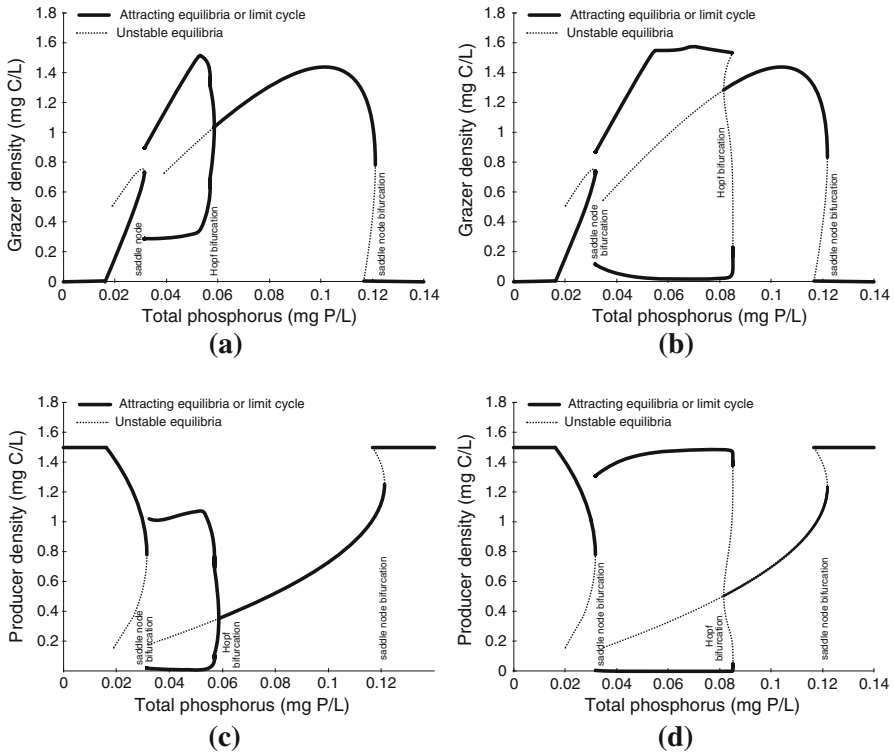


Fig. 4 Bifurcation diagrams for the knife-edge System (2) of the **a** grazer and **c** producer. Bifurcation diagrams for the full model System (15) of the **b** grazer and **d** producer. Parameter values are listed in Table 1. The bifurcation parameter, P , varies from 0 to 0.14 mg P/L. Data were generated using XPP-AUTO. Both diagrams have similar qualitative characteristics; however, there are some important differences between the two. Oscillations of the full model **b** exhibit much larger amplitudes than those of the knife-edge model **a**. Here, the fate of the grazer population is sensitive to stochastic extinction. The location of the Hopf bifurcation is different for these two models. The Hopf bifurcation of the knife-edge model **a** occurs at a lower value of P making the region where cycling occurs shorter and the region for stable coexistence longer. In the full model **b**, the Hopf bifurcation occurs at a higher value of P giving the grazer population a wider region of the dangerous limit cycling. After the Hopf bifurcation, the grazer population has a shorter window for the coexistence stable equilibrium before eventually going to extinction

population a wider region of the dangerous limit cycling. After the Hopf bifurcation, the grazer population has a shorter window for the coexistence stable equilibrium before eventually going to extinction. The location of the Hopf bifurcation depends on the parameters in the producer phosphorus uptake function (Eq. 6). The sensitivity of the bifurcation diagram to \hat{c} is shown in Fig. 5. The Hopf bifurcation point decreases as \hat{c} increases. It can be seen that the P bifurcation diagram of the full model converges to that of the two-dimensional model when \hat{c} and \hat{Q} are large enough.

The bifurcation diagrams suggest that the boundary grazer extinction equilibrium is stable for very low values of P , as well as very high values of P . These results correspond to the stability results stated in Theorems 3.3 and 3.4. The stability of the grazer extinction equilibrium, E_1 , depends on whether the grazer’s growth rate is

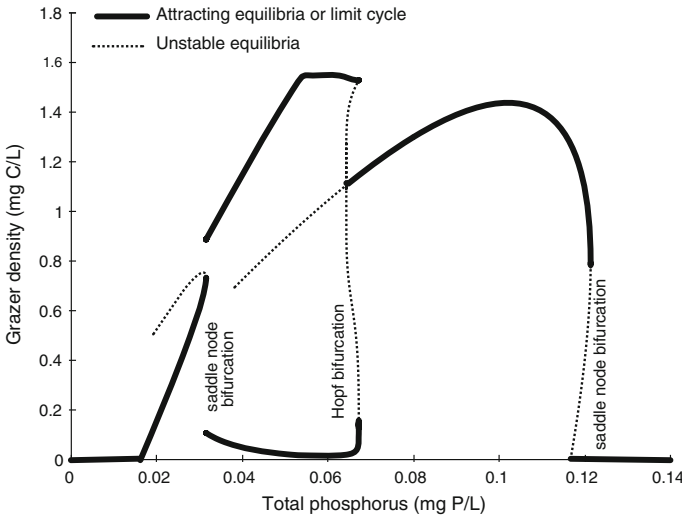


Fig. 5 Bifurcation diagrams for Full model System (15) using P as the bifurcation parameter with $\hat{c} = 0.8 \text{ mg P/mg C/d}$ and $\hat{Q} = 2.5 \text{ mg P/mg C}$. Data were generated using XPP-AUTO. Compare to Fig. 4b. Increasing \hat{c} effectively shifts the Hopf bifurcation to left, which decreases the region of periodic cycling and increases the region of the stable coexistence equilibrium

less than its death rate ($\min \left\{ \hat{e} f(x_1), \frac{Q_1}{\theta} f(x_1), \hat{e} \hat{f} \frac{\theta}{Q_1} \right\} < d$). Here, grazer’s growth is either determined by energy limitation ($\hat{e} f(x_1)$), P limitation ($\frac{Q_1}{\theta} f(x_1)$), or P in excess ($\hat{e} \hat{f} \frac{\theta}{Q_1}$). For very small values of P, x_1 and Q_1 are small and there is not enough P to support grazer’s growth. For very large values of P, Q_1 becomes large, so the producer P:C is too high to support grazer’s growth. In either case, the grazer dies out.

Figure 6 compares the bifurcation diagrams of three different producer–grazer models, the classical Rosenzweig–MacArthur variation in the Lotka–Volterra model (Rosenzweig and MacArthur 1963), the stoichiometric LKE model (System 1)(Loladze et al. 2000), and the knife-edge models (Systems 2, 15). The Rosenzweig–MacArthur exhibits a Hopf bifurcation and the “paradox of enrichment” (Rosenzweig 1971; Diehl 2007). Rather than simply increase grazer density, enrichment can lead to the destabilization of the steady state and increase risk of extinction. The “paradox of enrichment” is similarly exhibited by the LKE model. The stoichiometric constraints of low producer P:C on grazer growth incorporated into the LKE model introduces another paradox, the “paradox of energy enrichment” (Loladze et al. 2000; Diehl 2007). This is observed in the LKE bifurcation diagram past the blue line (Fig. 6b). Here, further enrichment in energy will actually decrease the grazer density. This is caused by low food quality, as the producer P:C is low and the grazer is limited by phosphorus. These two paradoxes, the “paradox of enrichment” and the “paradox of energy enrichment”, are also exhibited by the knife-edge models (Fig. 6c). Here, the bifurcation parameter is P, the total amount of phosphorus in the system. Unlike the other two bifurcation diagrams, which use K as the bifurcation diagram, here, producer P:C increases from left to right. The systems has similar a bifurcation sequence, but in the reverse order. The “paradox of energy enrichment” is exhibited in the region prior to the blue line

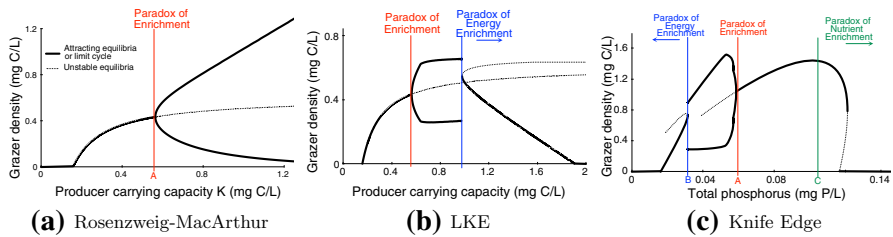


Fig. 6 Bifurcation diagrams for the Rosenzweig–MacArthur, the LKE model (System 1), and the knife-edge models (System 2, and System 15 with large \hat{c} , \hat{Q}). The bifurcation parameter for **a** and **b** is K , the producer carrying capacity in terms of carbon. The bifurcation parameter for the knife-edge model **c** is P , the total amount of phosphorus in the system. Data were generated using XPP-AUTO. Rosenzweig’s “paradox of enrichment” (Rosenzweig 1971; Diehl 2007) is seen in the Rosenzweig–MacArthur bifurcation diagram at the Hopf bifurcation (red line). Here, enrichment could lead to destabilization of the steady state and increased risk of extinction. This “paradox of enrichment” is also seen in the LKE bifurcation diagram (red line). The stoichiometric constraints incorporated into the LKE model introduce another paradox, the “paradox of energy enrichment” (Loladze et al. 2000; Diehl 2007). Energy enrichment past the blue line does not increase grazer density. Here, energy enrichment decreases grazer density. The bifurcation diagram for the knife-edge model uses nutrient enrichment instead of energy enrichment, so the system goes through the sequence of bifurcation in the reverse order. Producer P:C increases, rather than decreases, from left to right. The dynamics of the “paradox of enrichment” and the “paradox of energy enrichment” are seen in the red line and prior to the blue line. The effects of the stoichiometric knife edge introduce a third paradox to the model, the “paradox of nutrient enrichment”. This is seen when nutrient is enriched past the green line. Here the large amount of nutrients cause grazer density to decrease due to high producer P:C ratio. Extremely high nutrient enrichment will lead to grazer extinction (Color figure online)

in Fig. 6c. The dynamics of the “paradox of enrichment” are exhibited at the Hopf bifurcation at the red line. The effects of the stoichiometric knife edge introduce a third paradox to the model, and we will denote as the “paradox of nutrient enrichment”. Here, large amount of nutrients causes an increase in producer productivity, which causes an increase in producer density but does not result in an increase in grazer density. Grazer density starts to decrease due to high producer P:C ratio (green line in Fig. 6c). Extremely high nutrient enrichment can even lead to grazer extinction.

Nonintuitive paradoxes (“paradox of energy enrichment”, “paradox of nutrient enrichment”) arise when stoichiometric principles are incorporated into ecological models. Understanding these paradoxes will help shed light on population dynamics. Stiefs et al. (2010) investigated a generalized stoichiometric producer–grazer model and showed that increasing intraspecific competition has a stabilizing effect on the system. This motivated them to propose the “paradox of constraints”. Here, constraints on primary production aid the system by stabilizing the coexistent equilibrium. This concept of the “paradox of constraints” is exhibited in all three bifurcation diagrams in Fig. 6. In Fig. 6a, b, the “paradox of constraints” is seen at the Hopf bifurcations and corresponds with the “paradox of enrichment” (red line). If there was an energy constraint on these systems to keep the dynamics to the left of the Hopf bifurcation, the systems would remain stable and avoid oscillatory behaviors. The “paradox of constraints” is exhibited by the knife-edge model in Fig. 6c at the saddle-node bifurcation and corresponds with the “paradox of energy enrichment” (blue line). If there was a nutrient constraint on this system to keep the dynamics to the left of the saddle-node bifurcation, the system would remain stable and avoid oscillatory behaviors.

The full model (System (15)) is an extension of the nonsmooth stoichiometric LKE model (System (1)). Through a robust global analysis of the LKE model, Li et al. (2011) demonstrated that the LKE model has complicated dynamics including supercritical and subcritical Hopf bifurcations, saddle-node bifurcation, and transcritical bifurcation as well as a region of bistability with an interior equilibrium and limit cycles. We have shown that the full model exhibits some similar bifurcations and regions of bistability. Further analysis of interior equilibria and a rigorous bifurcation analysis may provide further insight and interesting dynamical behaviors.

While our model is built on empirical work related to zooplankton and algae dynamics and uses P as a key nutrient, it likely has broader applications. The “stoichiometric knife edge” has been observed in diverse situations (Hessen et al. 2013; Boersma and Elser 2006; Cease et al. 2012); however, the mechanisms underlying the knife edge are still not well understood. More studies are needed to better understand the effects of ranges of resource stoichiometry and the mechanism behind the reduction in grazer’s growth (Hessen et al. 2013).

The presented model makes the assumption that the θ , the P:C ratio of the grazer, is constant (A2). This strict homeostatic assumption is based on the fact that, although grazer stoichiometries are variable, the range of variation is small compared to the range of producer stoichiometries. Wang et al. (2012) investigated how the strict homeostatic assumption used in stoichiometric algae zooplankton models affects the dynamics. More work is needed to investigate the validity of (A2) and determine how varying θ changes the dynamics and predictions of this model.

Bifurcation analysis and numerical simulations of the full model, which explicitly tracks phosphorus, lead to quantitatively different predictions than previous models which neglect to track free nutrients. The full model provides better insight to the true effects that excess nutrients can have on the population dynamics of a food web. Since the previous model does not explicitly track free phosphorus, it underestimates the impacts that food quality can have on the growth of grazers. The full model shows that the fate of the grazer population is particularly sensitive to excess nutrient concentrations (Fig. 4). These results suggest that the *stoichiometric knife edge* phenomenon may play a larger role than originally predicted in previous models, especially when the producer maximum P per C uptake rate is low.

Acknowledgments This work was supported in part by NSF DMS-0920744 and NSERC Discovery Grant RES0001528. The authors thank two anonymous reviewers for their comments that improved this manuscript.

6 Appendix 1: Remaining Cases for Proof of Theorem 3.1

Proof Case 2: $x(t_1) = 0$
 Let $\bar{f} = f'(0) = \lim_{x \rightarrow 0} \frac{f(x)}{x}$ and $\bar{y} = \max_{t \in [0, t_1]} y(t) < \frac{P}{\theta}$. Then for every $t \in [0, t_1]$,

$$\begin{aligned}
 x' &= bx \min \left\{ 1 - \frac{x}{k}, 1 - \frac{q}{Q} \right\} - \min \left\{ f(x), \frac{\hat{f}\theta}{Q} \right\} y \\
 &\geq -f(x)y \geq -\bar{f}\bar{y}x \equiv \alpha x
 \end{aligned}$$

This implies that $x(t_1) \geq x(0)e^{\alpha t_1} > 0$, where α is a constant. This contradicts $x(t_1) = 0$ and proves that $S(t_1)$ does not reach this boundary.

Case 3: $y(t_1) = 0$

Then, for every $t \in [0, t_1]$,

$$y' = \min \left\{ \hat{e}f(x), \frac{Q}{\theta}f(x), \hat{e}\hat{f}\frac{\theta}{Q} \right\} y - dy \geq -dy.$$

This implies that $y(t_1) \geq y(0)e^{-dt_1} > 0$. This contradicts $y(t_1) = 0$ and proves that $S(t_1)$ does not reach this boundary.

Case 4: $Qx + \theta y = P$

Since $v(P - Q(t_1)x(t_1) - \theta y(t_1)) = 0$

$$\begin{aligned} \left. \frac{d(Qx + \theta y)}{dt} \right|_{t_1} &= Q'(t_1)x(t_1) + Q(t_1)x'(t_1) + \theta y'(t_1) \\ &= -Q(t_1) \min \left\{ f(x(t_1)), \frac{\hat{f}\theta}{Q(t_1)} \right\} y(t_1) \\ &\quad + \theta \min \left\{ \hat{e}f(x(t_1)), \frac{Q(t_1)}{\theta}f(x(t_1)), \hat{e}\hat{f}\frac{\theta}{Q(t_1)} \right\} y(t_1) - \theta dy(t_1) \\ &= -y(t_1) \min \left\{ f(x(t_1)), \frac{\hat{f}\theta}{Q(t_1)} \right\} \left(Q(t_1) - \theta \min \left\{ \hat{e}, \frac{Q(t_1)}{\theta} \right\} \right) \\ &\quad - \theta dy(t_1) \leq 0. \end{aligned}$$

Thus, $S(t_1)$ can not cross this boundary.

Case 5: $x(t_1) = K$

Then, for every $t \in [0, t_1]$,

$$\begin{aligned} x' &= bx \min \left\{ 1 - \frac{x}{k}, 1 - \frac{q}{Q} \right\} - \min \left\{ f(x), \frac{\hat{f}\theta}{Q} \right\} y \\ &\leq bx \min \left\{ 1 - \frac{x}{k}, 1 - \frac{q}{Q} \right\} \\ &= bx \left(1 - \frac{x}{\min \left\{ k, \frac{Qx}{q} \right\}} \right) \\ &\leq bx \left(1 - \frac{x}{\min \left\{ k, \frac{P}{q} \right\}} \right) \\ &= bx \left(1 - \frac{x}{K} \right). \end{aligned}$$

Then, $x(t_1) \leq K$ by a standard comparison argument, thus $S(t_1)$ can not cross this boundary.

Case 6: $Q(t_1) = \hat{Q}$

Since $v(P - Q(t_1)x(t_1) - \theta y(t_1), Q(t_1)) = 0$

$$Q' = -b \min \left\{ Q \left(1 - \frac{x}{k} \right), Q - q \right\} < 0.$$

Thus, $S(t_1)$ can not cross this boundary. □

7 Appendix 2: Proof of Theorem 3.2

Proof To prove that E_0 is unstable, it is sufficient to show the system linearized at this equilibrium has an eigenvalue whose real part is positive. This is seen in the following Jacobian,

$$J(E_0) = \begin{vmatrix} b \left(1 - \frac{q}{Q_0} \right) & 0 & 0 \\ 0 & G(0, 0, Q_0) & 0 \\ H_x(0, 0, Q_0) & H_y(0, 0, Q_0) & H_Q(0, 0, Q_0) \end{vmatrix},$$

where $b \left(1 - \frac{q}{Q_0} \right) > 0$. □

8 Appendix 3: Proof of Lemma 3.1

Proof We consider two cases $(1 - \frac{x}{k} < 1 - \frac{q}{Q}$ and $1 - \frac{x}{k} > 1 - \frac{q}{Q})$.

Case 1: $1 - \frac{x}{k} < 1 - \frac{q}{Q}$ In this case, (Eq. 15a) becomes

$$\frac{dx}{dt} = bx \left(1 - \frac{x}{k} \right) - \min \left\{ f(x), \frac{\hat{f}\theta}{Q} \right\} y \tag{21}$$

and $x_1 = k$. (Eq. 15c) becomes

$$\frac{dQ}{dt} = v(P - Qx - \theta y, Q) - bQ \left(1 - \frac{x}{k} \right) \tag{22}$$

therefore, $v(P - Q_1k, Q_1) = 0$. There are two cases to consider here ($\frac{P}{k} > \hat{Q}$ and $\frac{P}{k} < \hat{Q}$). If $\frac{P}{k} > \hat{Q}$, then $Q_1 = \hat{Q}$ to remain in Ω . Since $P \geq Q_1x_1 = Q_1k$, the case when $\frac{P}{k} < \hat{Q}$ results in $\hat{Q} > \frac{P}{k} \geq Q_1$, thus $Q_1 = \frac{P}{k}$. The two cases are summarized below

$$Q_1 = \left\{ \begin{matrix} \hat{Q} & \text{if } \frac{P}{k} > \hat{Q} \\ \frac{P}{k} & \text{if } \frac{P}{k} < \hat{Q} \end{matrix} \right\} = \min \left\{ \frac{P}{k}, \hat{Q} \right\}. \tag{23}$$

Case 2: $1 - \frac{x}{k} > 1 - \frac{q}{Q}$
 In this case, (Eq. 15a) becomes

$$\frac{dx}{dt} = bx \left(1 - \frac{q}{Q} \right) - \min \left\{ f(x), \frac{\hat{f}\theta}{Q} \right\} y \tag{24}$$

and $Q_1 = q$. (Eq. 15c) becomes

$$\frac{dQ}{dt} = v(P - Qx - \theta y, Q) - bQ \left(1 - \frac{q}{Q} \right) \tag{25}$$

therefore $v(P - qx_1, q) = 0$ and thus $x_1 = \frac{P}{q}$.

To show that the two equilibrium forms cannot coexist, we need to show that they satisfy two opposite conditions.

In case 1: $1 - \frac{x}{k} < 1 - \frac{q}{Q}$ and $E_1 = \left(k, 0, \min \left\{ \frac{P}{k}, \hat{Q} \right\} \right)$, therefore

$$\begin{aligned} 0 &< 1 - \frac{q}{\min \left\{ \frac{P}{k}, \hat{Q} \right\}} \\ \implies \min \left\{ \frac{P}{k}, \hat{Q} \right\} &> q. \end{aligned}$$

Here

$$\frac{P}{k} \geq \min \left\{ \frac{P}{k}, \hat{Q} \right\} > q.$$

In case 2: $1 - \frac{x}{k} > 1 - \frac{q}{Q}$ and $E_1 = \left(\frac{P}{q}, 0, q \right)$, therefore

$$\begin{aligned} 1 - \frac{P}{qk} &> 0 \\ \implies \frac{P}{k} &< q. \end{aligned}$$

The two cases follow opposite conditions. Actually, when $\frac{P}{k} = q$, the two forms of E_1 collide to $(k, 0, q)$. □

9 Appendix 4: Proof of Theorem 3.3

Proof Assume that $\min \left\{ \hat{e}f(x_1), \frac{Q_1}{\theta} f(x_1), \hat{e}\hat{f}\frac{\theta}{Q_1} \right\} < d$. To prove that E_1 is stable, we consider two cases ($1 - \frac{x}{k} < 1 - \frac{q}{Q}$ and $1 - \frac{x}{k} > 1 - \frac{q}{Q}$) where we look at the linearized system and use the Routh–Hurwitz criterion.

Case 1: $1 - \frac{x}{k} < 1 - \frac{q}{Q}$

Here, $E_1 = \left(k, 0, \min \left\{ \frac{P}{k}, \hat{Q} \right\} \right)$ by Lemma 3.1 and the Jacobian takes the following form,

$$J(E_1) = \begin{vmatrix} -b & kF_y \left(k, 0, \min \left\{ \frac{P}{k}, \hat{Q} \right\} \right) & 0 \\ 0 & \min \left\{ \hat{e}f(k), \frac{\min \left\{ \frac{P}{k}, \hat{Q} \right\}}{\theta} f(k), \hat{e} \hat{f} \frac{\theta}{\min \left\{ \frac{P}{k}, \hat{Q} \right\}} \right\} - d & 0 \\ H_x \left(k, 0, \min \left\{ \frac{P}{k}, \hat{Q} \right\} \right) & H_y \left(k, 0, \min \left\{ \frac{P}{k}, \hat{Q} \right\} \right) & \frac{dv}{dQ} \Big|_{E_1} \end{vmatrix}.$$

Let $\alpha_1 = \min \left\{ \hat{e}f(k), \frac{\min \left\{ \frac{P}{k}, \hat{Q} \right\}}{\theta} f(k), \hat{e} \hat{f} \frac{\theta}{\min \left\{ \frac{P}{k}, \hat{Q} \right\}} \right\} - d < 0$ and $\alpha_2 = \frac{dv}{dQ} \Big|_{E_1} < 0$.

Then, the Jacobian simplifies to

$$J(E_1) = \begin{vmatrix} -b & kF_y \left(k, 0, \min \left\{ \frac{P}{k}, \hat{Q} \right\} \right) & 0 \\ 0 & \alpha_1 & 0 \\ H_x \left(k, 0, \min \left\{ \frac{P}{k}, \hat{Q} \right\} \right) & H_y \left(k, 0, \min \left\{ \frac{P}{k}, \hat{Q} \right\} \right) & \alpha_2 \end{vmatrix}.$$

The characteristic equation may be written

$$(-b - \lambda)(\alpha_1 - \lambda)(\alpha_2 - \lambda) = 0$$

The eigenvalues of $J(E_1)$ are $-b, \alpha_1, \alpha_2$, which are all negative.

Case 2: $1 - \frac{x}{k} > 1 - \frac{q}{Q}$

Here, $E_1 = \left(\frac{P}{q}, 0, q\right)$ by Lemma 3.1 and the Jacobian takes the following form,

$$J(E_1) = \begin{vmatrix} 0 & \frac{P}{q} F_y \left(\frac{P}{q}, 0, q\right) & \frac{Pb}{q^2} \\ 0 & \min \left\{ \hat{e}f\left(\frac{P}{q}\right), \frac{\hat{q}}{\theta} f\left(\frac{P}{q}\right), \hat{e} \hat{f} \frac{\theta}{q} \right\} - d & 0 \\ \frac{dv}{dx} \Big|_{E_1} & H_y \left(\frac{P}{q}, 0, q\right) & \frac{dv}{dQ} \Big|_{E_1} - b \end{vmatrix}.$$

Let $\alpha_1 = \min \left\{ \hat{e}f\left(\frac{P}{q}\right), \frac{\hat{q}}{\theta} f\left(\frac{P}{q}\right), \hat{e} \hat{f} \frac{\theta}{q} \right\} - d < 0, \alpha_2 = \frac{dv}{dQ} \Big|_{E_1} - b < 0, \alpha_3 = \frac{dv}{dx} \Big|_{E_1} < 0$. Then the Jacobian simplifies down to

$$J(E_1) = \begin{vmatrix} 0 & \frac{P}{q} F_y \left(\frac{P}{q}, 0, q\right) & \frac{Pb}{q^2} \\ 0 & \alpha_1 & 0 \\ \alpha_3 & H_y \left(\frac{P}{q}, 0, q\right) & \alpha_2 \end{vmatrix}.$$

The characteristic equation may be written

$$\lambda^3 + \lambda^2(-\alpha_1 - \alpha_2) + \lambda(\alpha_1\alpha_2 - \frac{Pb}{q^2}\alpha_3) + \frac{Pb}{q^2}\alpha_1\alpha_3.$$

Since $\alpha_1, \alpha_2, \alpha_3 < 0$ we find that $-\alpha_1 - \alpha_2 > 0$, $\frac{Pb}{q^2}\alpha_1\alpha_3 > 0$, and $(-\alpha_1 - \alpha_2)(\alpha_1\alpha_2 - \frac{Pb}{q^2}\alpha_3) > \frac{Pb}{q^2}\alpha_1\alpha_3$. These are the conditions of the Routh–Hurwitz criterion that guarantee all the eigenvalues of $J(E_1)$ have strictly negative real parts. Thus, E_1 is locally asymptotically stable for both cases. \square

10 Appendix 5: Proof of Theorem 3.4

Proof The set Ω is positively invariant under System (15) by Lemma 3.1. Let

$$\alpha = \min \left\{ \hat{e}f(K), \frac{\hat{Q}}{\theta}f(K), \hat{e}\hat{f}\frac{\theta}{q} \right\} - d < 0. \tag{26}$$

For all $(x, y, Q) \in \Omega$, the expression for y' may be expressed as

$$\begin{aligned} \frac{y'}{y} &= \min \left\{ \hat{e}f(x), \frac{Q}{\theta}f(x), \hat{e}\hat{f}\frac{\theta}{Q} \right\} - d \\ &\leq \min \left\{ \hat{e}f(K), \frac{\hat{Q}}{\theta}f(K), \hat{e}\hat{f}\frac{\theta}{q} \right\} - d \\ &= \alpha \end{aligned}$$

This implies that $\lim_{t \rightarrow \infty} y(t) = 0$. In autonomous System (15), $y(t)$ converges to 0. We may consider the behavior of System (15) on the plane $y = 0$ with the limit system

$$\frac{dx}{dt} = bx \min \left\{ 1 - \frac{x}{k}, 1 - \frac{q}{Q} \right\} \tag{27a}$$

$$\frac{dQ}{dt} = v(P - Qx, Q) - b \min \left\{ Q\left(1 - \frac{x}{k}\right), (Q - q) \right\}, \tag{27b}$$

defined on the domain

$$\bar{\Omega} = \left\{ (x, Q) \mid 0 < x < K, q < Q < \hat{Q} \right\} \tag{28}$$

System (27) is the limiting system of the asymptotically autonomous System (15) under the constraint $\min \left\{ \hat{e}f(K), \frac{\hat{Q}}{\theta}f(K), \hat{e}\hat{f}\frac{\theta}{q} \right\} - d$. Results from Markus (1956) and Thieme (1992) allow us to compare solutions of an autonomous system with those of the asymptotically autonomous limit system. System (27) has one equilibrium $\bar{E}_1 = (\bar{x}_1, \bar{Q}_1)$, and this equilibrium is globally asymptotically stable. To show this global stability, we consider two cases $(1 - \frac{x}{k} < 1 - \frac{q}{Q}$ and $1 - \frac{x}{k} > 1 - \frac{q}{Q})$ where we look at the linearized system and then consider the existence of periodic orbits.

Case 1: $1 - \frac{x}{k} < 1 - \frac{q}{Q}$

Here, $\bar{E}_1 = \left(k, \min \left\{ \frac{P}{k}, \hat{Q} \right\} \right)$ and the Jacobian takes the form,

$$J(\bar{E}_1) = \begin{vmatrix} -b & 0 \\ \frac{dv}{dx}|_{\bar{E}_1} + \frac{b \min \left\{ \frac{P}{k}, \hat{Q} \right\}}{k} & \frac{dv}{dQ}|_{\bar{E}_1} \end{vmatrix}.$$

The eigenvalues are $-b < 0$ and $\frac{dv}{dQ}|_{\bar{E}_1} < 0$.

Case 2: $1 - \frac{x}{k} > 1 - \frac{q}{Q}$

Here, $\bar{E}_1 = \left(\frac{P}{q}, q\right)$ and the Jacobian takes the form,

$$J(\bar{E}_1) = \begin{vmatrix} 0 & b \frac{P}{q^2} \\ \frac{dv}{dx}|_{\bar{E}_1} & \frac{dv}{dQ}|_{\bar{E}_1} - b \end{vmatrix}.$$

Here, $\text{trace}(J(\bar{E}_1)) = \frac{dv}{dQ}|_{\bar{E}_1} - b < 0$ and $\text{det}(J(\bar{E}_1)) = -b \frac{P^2}{q^2} \frac{dv}{dx}|_{\bar{E}_1} > 0$. In both cases, \bar{E}_1 is locally asymptotically stable. To show that no periodic orbits exist in $\bar{\Omega}$, consider

$$(xQ)' = xv(P - Qx, Q) > 0.$$

Therefore, there is no t_1 such that $Q'(t_1) < 0$ and $x'(t_1) < 0$; hence, there can not be any periodic solutions. Since $\bar{\Omega}$ is simply connected and is positively invariant under System (27) and contains no periodic orbits, by the Poincaré–Bendixson Theorem, all solutions of System (27) starting in $\bar{\Omega}$ will converge to \bar{E}_1 . Thus, \bar{E}_1 is globally asymptotically stable. The ω -limit set of a forward bounded solution of the autonomous System (15) consists of the equilibrium of its limit autonomous System (27) (Thieme 1992). Thus, the ω -limit set of System (15) is $\{E_1\}$. The grazer only extinction equilibrium E_1 is globally asymptotically stable,

$$\begin{aligned} \text{if } 1 - \frac{x}{k} < 1 - \frac{q}{Q} \text{ then } \lim_{t \rightarrow \infty} (x(t), y(t), Q(t)) &= \left(k, 0, \min \left\{ \frac{P}{k}, \hat{Q} \right\} \right), \\ \text{if } 1 - \frac{x}{k} > 1 - \frac{q}{Q} \text{ then } \lim_{t \rightarrow \infty} (x(t), y(t), Q(t)) &= \left(\frac{P}{q}, 0, q\right). \end{aligned}$$

□

11 Appendix 6: Supplementary Material Notes

An animation of the three dimensional phase space is provided in the supplementary material. The animation was created using MATLAB. Here, we used the Holling-type II function $f(x) = \frac{\hat{f}x}{a+x}$ for the grazer ingestion rate and the parameter values listed in Table 1 and P varying from 0.001 to 0.14 mg P/L. The surfaces are the producer (blue), grazer (yellow), and producer P:C (red) nullsurfaces. The intersections of these

surfaces depict equilibria. The equilibria that simulations suggest are stable are labeled with black dots; equilibria that simulations suggest are unstable are labeled with white dots.

References

- Andersen T (1997) Pelagic nutrient cycles: herbivores as sources and sinks. Springer, New York
- Bennett EM, Carpenter SR, Caraco NF (2001) Human impact on erodable phosphorus and eutrophication: a global perspective. *Bioscience* 51(3):227–234
- Boersma M, Elser J (2006) Too much of a good thing: on stoichiometrically balanced diets and maximal growth. *Ecology* 87:1325–1330
- Cease A, Elser J, Ford C, Hao S, Kang L, JF H (2012) Heavy livestock grazing promotes locust outbreaks by lowering plant nitrogen content. *Science* 335:467–469
- Demott W, Gulati R, Siewertsen K (1998) Effects of phosphorus-deficient diets on the carbon and phosphorus balance of *Daphnia magna*. *Limnol Oceanogr* 43:1147–1161
- Diehl S (2007) Paradoxes of enrichment: effects of increased light versus nutrient supply on pelagic producer–grazer systems. *Am Nat* 169(6):E173–E191
- Elser J, Bennett E (2011) Phosphorus cycle: a broken biogeochemical cycle. *Nature* 478:29–31
- Elser J, Hayakawa K, Urabe J (2001) Nutrient limitation reduces food quality for zooplankton: *Daphnia* response to seston phosphorus enrichment. *Ecology* 82:898–903
- Elser J, Watts J, Schampell J, Farmer J (2006) Early Cambrian food webs on a trophic knife-edge? A hypothesis and preliminary data from a modern stromatolite-based ecosystem. *Ecol Lett* 9:295–303
- Elser JJ, Loladze I, Peace AL, Kuang Y (2012) Lotka re-loaded: modeling trophic interactions under stoichiometric constraints. *Ecol Model* 245:3–11
- Frost P, Benstead J, Cross W, Hillebrand H, Larson J, Xenopoulos M, Yoshida T (2006) Threshold elemental ratios of carbon and phosphorus in aquatic consumers. *Ecol Lett* 9:774–779
- Gaxiola RA, Edwards M, Elser JJ (2011) A transgenic approach to enhance phosphorus use efficiency in crops as part of a comprehensive strategy for sustainable agriculture. *Chemosphere* 84(6):840–845
- Hessen DO, Elser JJ, Sterner RW, Urabe J (2013) Ecological stoichiometry: an elementary approach using basic principles. *Limnol Oceanogr* 58(6):2219–2236
- Li X, Wang H, Kuang Y (2011) Global analysis of a stoichiometric producer–grazer model with holling type functional responses. *J Math Biol* 63(5):901–932
- Loladze I, Kuang Y, Elser J (2000) Stoichiometry in producer–grazer systems: linking energy flow with element cycling. *Bull Math Biol* 62:1137–1162
- Markus L (1956) Asymptotically autonomous differential systems. In: Contributions to the theory of non-linear oscillations III, vol 36, pp 17–29
- Peace A, Zhao Y, Loladze I, Elser JJ, Kuang Y (2013) A stoichiometric producer–grazer model incorporating the effects of excess food-nutrient content on consumer dynamics. *Math Biosci* 244(2):107–115
- Rosenzweig ML (1971) Paradox of enrichment: destabilization of exploitation ecosystems in ecological time. *Science* 171(3969):385–387
- Rosenzweig ML, MacArthur RH (1963) Graphical representation and stability conditions of predator–prey interactions. *Am Nat* 97(895):209
- Smith V, Schindler D (2009) Eutrophication science: where do we go from here? *Trends Ecol Evol* 24:201–207
- Sterner RW, Andersen T, Elser JJ, Hessen DO, Hood JM, McCauley E, Urabe J (2008) Scale-dependent carbon: nitrogen: phosphorus seston stoichiometry in marine and freshwaters. *Limnol Oceanogr* 53(3):1169
- Stiefs D, Van Voorn GA, Kooi BW, Feudel U, Gross T (2010) Food quality in producer–grazer models: a generalized analysis. *Am Nat* 176(3):367–380
- Thieme HR (1992) Convergence results and a poincaré-bendixson trichotomy for asymptotically autonomous differential equations. *J Math Biol* 30(7):755–763
- Urabe J, Sterner RW (1996) Regulation of herbivore growth by the balance of light and nutrients. *Proc Nat Acad Sci* 93(16):8465–8469
- Wang H, Kuang Y, Loladze I (2008) Dynamics of a mechanically derived stoichiometric producer–grazer model. *J Biol Dyn* 2(3):286–296
- Wang H, Sterner RW, Elser JJ (2012) On the strict homeostasis assumption in ecological stoichiometry. *Ecol Model* 243:81–88